



SYNTHESIS, QSAR ANALYSIS AND MOLECULAR DOCKING STUDIES OF FLAVONE HYDRAZIDE SULFONYL DERIVATIVES AS DIABETIC INHIBITORS

Javeria Shaikh^{a*}, Waqas Jamil^a, Sehar Zahid^{a,b}, Samreen Zainalabdin^a

^aInstitute of Advanced Research Studies in Chemical Sciences, University of Sindh, Jamshoro

^bDr.M.A.Kazi Institute of Chemistry, University of Sindh, Jamshoro

***Corresponding Author:-** Javeria Shaikh

^{*}Institute of Advanced Research Studies in Chemical Sciences, University of Sindh, Jamshoro

Abstract

Flavone Hydrazide Sulfonyl derivatives **1-20** has synthesized and structural properties has confirmed by spectroscopic techniques. These compounds were also found to be active against α -glucosidase enzyme. Among these, Compound **6** ($IC_{50}=7.5 \pm 1.98\mu M$), **9** ($IC_{50}=9.2 \pm 1.87\mu M$) and **4** ($IC_{50}=9.3 \pm 1.67\mu M$) showed marvelous inhibition activity.

All the synthesized compounds were subject for *in silico* studies.

The molecular docking analysis revealed that these molecules have high potential to interact with the enzyme. According to the physicochemical and pharmacokinetics studies these compound have excellent parameters required for drug likeness. The derivatives have ability of GI absorption. In addition, all the synthesized Flavone Hydrazide derivatives **1-20** were also evaluated for their antioxidant (DPPH Radical scavenging) activity. All these computed showed very promising antioxidant activity IC_{50} ranges 15.25-58.38 μM respectively.

1. Introduction

Diabetes mellitus (DM) is a global disease that poses a public health threat [1]. It is on the rise, and the World Health Organization projects that by 2030, diabetes will be the sixth biggest cause of death worldwide [2], [3]. It is a metabolic condition in which blood glucose levels rise as a result of abnormalities in insulin action, production, or both (insulin is insufficient or inefficient). Its impacted around 415 million people aged 20 to 79 in 2015, according to the International Diabetes Federation (IDF). By 2040, another 200 million individuals are anticipated to be impacted by DM, making it a global public health problem [4].

Type 1 diabetes, type 2 diabetes, and gestational diabetes are the three forms of diabetes based on a etiology and clinical presentation (GDM) [5].

Type 1 diabetes mellitus (T1DM) is defined by the autoimmune destruction of insulin-producing beta cells in the pancreatic islets, accounting for 5% to 10% of all diabetes cases. As a result, there is an absolute insulin shortage. Autoimmunity has been linked to a mix of genetic susceptibility and

environmental influences such as viral infection, toxins, and certain dietary factors. T1DM most typically affects children and teenager, however it can affect anyone at any age [6].

T2DM (type 2 diabetes mellitus) accounts for almost 90% of all diabetes cases. Insulin resistance is described as a reduced response to insulin in people with T2DM. Insulin is inefficient in this state; hence an increase in insulin synthesis is used to maintain glucose homeostasis. However, insulin production diminishes with time, culminating in T2DM. T2DM is most typically found in those over the age of 45. Despite this, because to increased levels of obesity, physical inactivity, and energydense meals, it is becoming more common in children, adolescents, and younger people [7]. Gestational diabetes mellitus (GDM), commonly known as hyperglycemia in pregnancy, is a type of hyperglycemia that first appears during pregnancy [8].

Inhibition of digestive enzymes like α -amylase and α -glucosidase has long been thought to be a good way to regulate blood sugar. Reducing post-prandial hyperglycemia can be achieved by delaying the activity of the enzymes α -amylase and α -glucosidase, which are responsible for carbohydrate digestion and glucose absorption in the digestive system, respectively [9][10]. Figure 1 shows Metabolizes Disaccharides into Monosaccharides.



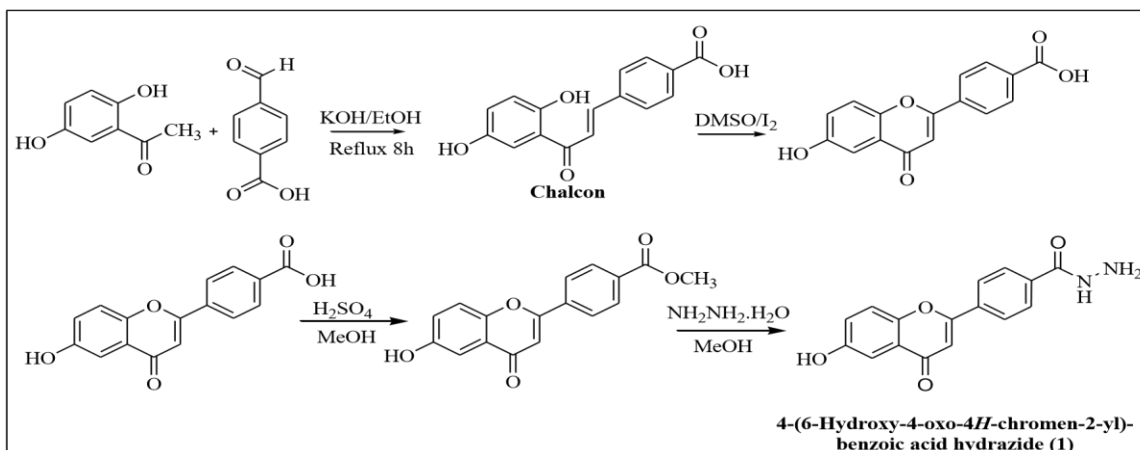
Figure 1: Metabolizes Disaccharides into Monosaccharides

The enzyme inhibitors Acarbose, Miglitol, and Voglibose are now used to regulate PPHG. Certain medications may work by inhibiting or blocking these enzymes [11]. Miglitol and Voglibose inhibit solely α -glucosidase, while Acarbose inhibits both α -amylase and α -glucosidase. These inhibitors are successful at controlling PPHG, but their gastrointestinal side effects make them unsuitable for longterm use [12].

2. Chemistry

2.1. Synthesis of flavone hydrazide

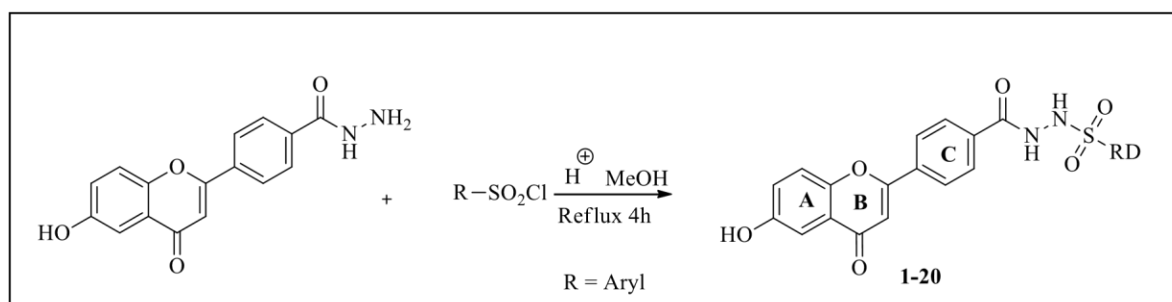
The key intermediate 4-(6-hydroxy-4-oxo-4H-benzopyran-2-yl)-benzoic acid hydrazide (Flavone hydrazide) was synthesized in four (4)-steps. Synthesis of chalcone is the step first. Chalcone was synthesized by treating 2,5-dihydroxy acetophenone with 4-formylbenzoic acid in the presence of ethanolic potassium hydroxide. In second step, the cyclization of chalcone via I2/DMSO methodology was done. In this step, oxidative cyclization of chalcone was done in order to obtain flavone carboxylic acid derivative. In third step, the flavone carboxylic acid derivative was further refluxed with methanol/sulphuric acid mixture to convert the flavone carboxylic acid into flavone ester. In fourth step, this flavone methyl ester was reacted with hydrazine hydrate in order to obtain the target flavone hydrazide (Scheme 1). The structure of target molecule was confirmed by H1 NMR, C13NMR and Elemental (CHN/S) analysis.



Scheme 1. Reaction for the synthesis of 4-(6-Hydroxy-4-oxo-4H-chromen-2-yl)-benzoic acid hydrazone

2.2. SYNTHESIS OF FLAVONE HYDRAZIDE SULFONYL DERIVATIVES 1-20

4-(6-Hydroxy-4-oxo-4H-chromen-2-yl)-benzoic acid hydrazone (Flavone hydrazone) was refluxed with various aryl aldehydes/ketones in the presence of acetic acid (Figure 4.48). The structures of Flavone hydrazone. Sulfonyl derivatives 1-20 was established according to the HNMR, Elemental analysis and CHN/S analysis.



Scheme 2. Synthesis of Flavone Hydrazone Sulfonyl Schiff Base Derivatives 1-20

3. Result and discussion

3.1. α -Glucosidase Enzyme Inhibition Activity

All the synthesized derivatives **1-20** were subjected for the evaluation of α -glucosidase inhibition activity in order to explore anti-diabetic activity of these compounds.

The results were compared with standard acarbose ($IC_{50} = 39.45 \pm 0.11 \mu M$). All these compounds showed very promising α -glucosidase inhibition activity IC_{50} ranges 1.02- 38.1 μM and found to be better active than the standard acarbose.

The -OH group containing compounds **4** ($IC_{50} = 9.3 \pm 1.67 \mu M$), **5** ($IC_{50} = 11.7 \pm 1.34 \mu M$), **6** ($IC_{50} = 7.5 \pm 1.98 \mu M$), better activity among their look likes. The highest activity shown by compound **6** ($IC_{50} = 7.5 \pm 1.98 \mu M$). While 3rd most active compound **4** ($IC_{50} = 9.3 \pm 1.67 \mu M$). The chloro (-Cl) substituted compounds **1** ($IC_{50} = 20.4 \pm 0.95 \mu M$), **2** ($IC_{50} = 23.7 \pm 1.13 \mu M$), **3** ($IC_{50} = 13.3 \pm 1.21 \mu M$) and **10** ($IC_{50} = 11.4 \pm 1.64 \mu M$) also showed significant activity towards α -glucosidase inhibition. All these compounds showed better activity than the standard. The -NO₂ group substituted compounds **7** ($IC_{50} = 34.1 \pm 0.87 \mu M$), **8** ($IC_{50} = 38.4 \pm 1.12 \mu M$), **9** ($IC_{50} = 27.6 \pm 1.36 \mu M$) were also found to be better active than the standard but relatively they showed less activity than -OH group containing analogues. The less activity might be due to reducing number of hydrogen bonding interaction sites or larger size of -NO₂ group than the -OH group. Compound containing -CH₃ and OCH₃ group substituted **15** ($IC_{50} = 51.1 \pm 1.23 \mu M$), **16** ($IC_{50} = 47.6 \pm 1.84 \mu M$) and **18** ($IC_{50} = 45.5 \pm 1.66 \mu M$) show slightly less active than the standard. The heterocyclic ring containing compounds **13** ($IC_{50} =$

$34.1 \pm 1.32\mu\text{M}$) and **14** ($\text{IC}_{50} = 26.2 \pm 1.67\mu\text{M}$) showed better activity and they were also found to be better active than the standard but compound **17** ($\text{IC}_{50} = 49.2 \pm 1.45\mu\text{M}$) showed less active than standard. The halogen containing compounds **11** ($\text{IC}_{50} = 29.3 \pm 1.33\mu\text{M}$) and **12** ($\text{IC}_{50} = 9.2 \pm 1.87\mu\text{M}$) showed better activity and they were also found to be better active than the standard.

Table 1: R Group Representation

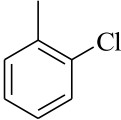
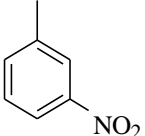
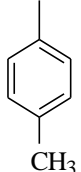
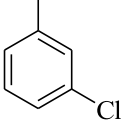
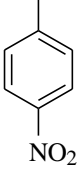
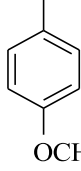
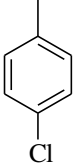
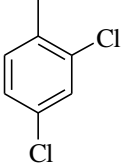
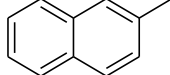
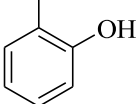
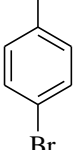
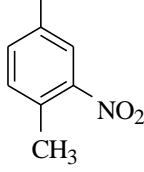
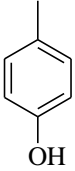
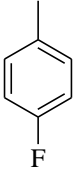
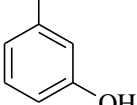
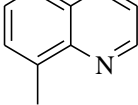
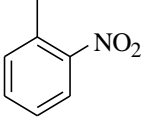
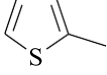
S.#	R	S.#	R	S.#	R
1.		8.		15.	
2.		9.		16.	
3.		10.		17.	
4.		11.		18.	
5.		12.		19.	CH ₃ -
6.		13.		20.	CH ₃ -CH ₂
7.		14.			

Table 2: α -Glucosidase Inhibition Activity of Compounds 1-20

S.#	IC ₅₀ μ M \pm SEMa	S.#	IC ₅₀ μ M \pm SEMa
1.	20.4 \pm 0.95	11.	29.3 \pm 1.33
2.	23.7 \pm 1.13	12.	9.2 \pm 1.87
3.	13.3 \pm 1.21	13.	34.1 \pm 1.32
4.	9.3 \pm 1.67	14.	26.2 \pm 1.67
5.	11.7 \pm 1.34	15.	51.1 \pm 1.23
6.	7.5 \pm 1.98	16.	47.6 \pm 1.84
7.	34.1 \pm 0.87	17.	49.2 \pm 1.45
8.	38.4 \pm 1.12	18.	45.5 \pm 1.66
9.	27.6 \pm 1.36	19.	53.1 \pm 1.34
10.	11.4 \pm 1.64	20.	50.3 \pm 1.83
	Acarbose (Standard)		39.45 \pm 0.11

4. Computational Analysis

4.1. Homology modeling of α -glucosidase enzyme

With the aid of the homology modeling technique, the 3D structure of the enzyme α -glucosidase from *Saccharomyces cerevisiae* (Baker's yeast) was developed. (PDB ID: 3A4A; Supporting Information).

4.2. Molecular docking analysis

In order to comprehend the binding interaction of the synthetic compounds **1-20** with α -glucosidase enzyme, molecular docking was performed on the most active compounds **4-6**, and **12**. The binding affinity for each prepared ligand against prepared α -glucosidase enzyme was calculated using AutoDock Vina (version 1.2.0)[13], [14], limiting the energy range of 3 and exhaustiveness of 8 against 9 best docking poses. All four synthetic analogs showed good non-bonding interactions within the binding pocket of the receptor, as represent in Figure 2.

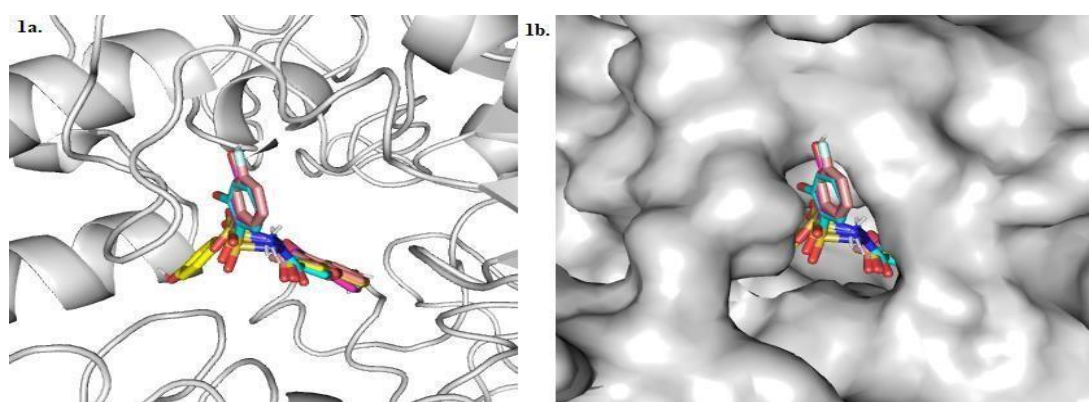


Figure 2: (a) Cartoon representation of active site of α -glucosidase (b) Binding cavity of α glucosidase

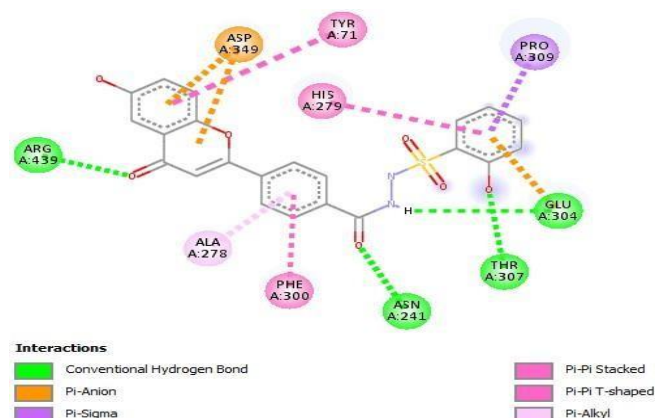


Figure 3: 2D plot of non-bonding interactions compound **4** within active site of α -glucosidase

Compound **4** is found to be the second most potent inhibitor of series with ($IC_{50} = 9.3 \pm 1.67 \mu M$). The dock pose analysis of the compound **4** is showing interaction *via* H-bonding with the amino acids ARG 439, Asn 241, Thr 307 Glu 304 with the carbonyl and $-OH$ group, however T-shaped and

parallel, π - π stacking interactions are also possibly existing with PHE A 300, HIS A 279, TYR A 71, as shown in Figure 4.

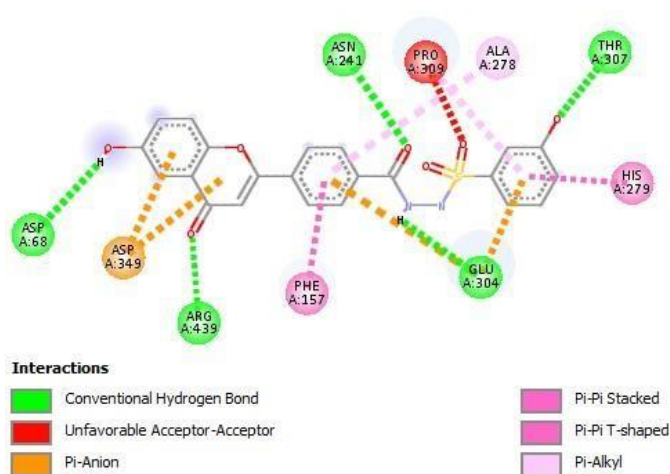


Figure 4: 2D plot of non-bonding interactions compound **5** within active site of α -glucosidase. Compound **5** is found to be the fifth most potent inhibitor of series with ($IC_{50} = 11.7 \pm 1.34 \mu M$) comparative to standard drug acarbose ($IC_{50} = 39.45 \pm 0.11 \mu M$). The dock pose analysis of the compound is showing interaction *via* H-bonding with the amino acids ASP 68, ASN 241, THR 307, GLU 304 and ARG 439 with the carbonyl and $-OH$ group, however T-shaped and parallel, π - π stacking interactions are also possibly existing with PHE 157, HIS 279, as shown in Figure 4.

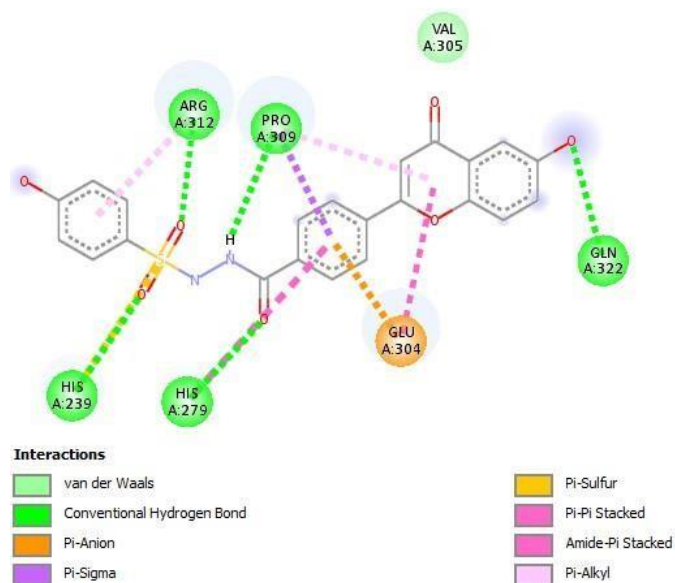


Figure 5: 2D plot of non-bonding interactions compound **6** within active site of α -glucosidase

Compound **6** is found to be the most potent inhibitor of series with ($IC_{50} = 7.5 \pm 1.98 \mu M$) almost 25 times more potent inhibitor comparative to standard drug acarbose ($IC_{50} = 39.45 \pm 0.11 \mu M$). The dock pose analysis of the compound is showing interaction *via* Vander Waals and H-bonding with the amino acids HIS 239, HIS 279, GLU 322 with the carbonyl and $-OH$ group, however π -Anion interactions are also possibly existing with GLU 304, as shown in Figure 5.

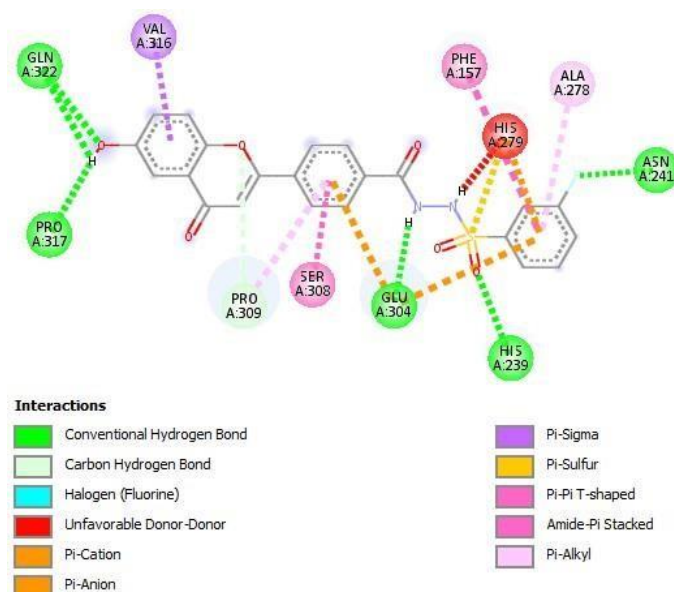


Figure 6: 2D plot of non-bonding interactions compound **12** within active site of α -glucosidase

Compound **12** is found to be the third most potent inhibitor of series with ($IC_{50} = 9.2 \pm 1.87 \mu M$) comparative to standard drug acarbose ($IC_{50} = 39.45 \pm 0.11 \mu M$), The dock pose analysis of the compound is showing interaction *via* H-bonding with the amino acids ASN 241, GLN 322, PRO 317 HIS 239 and GLU 304 with the carbonyl and -OH group, however π - π T-shaped interactions are also possibly existing with SER 308, PHE 157, as shown in Figure 6.

4.3. H^1 NMR C^{13} NMR AND ESI AND ELEMENTAL (CHN/S) ANALYSIS

4.3.1 4-(6-HYDROXY-4-OXO-4H-CHROMEN-2-YL)-BENZOIC ACID (2,4-DIHYDROXY-BENZYLIDENE)-HYDRAZIDE **1**

M.P. 302°C; Solid; Yield: 83%; 1H NMR (300MHz, DMSO- d_6): 2.0 (s, 1H) 7.87 (s, 1H), 7.52 (s, 1H), 7.56 (s, 1H), 6.76 (s, 1H), 7.23 (s, 1H), 6.84 (s, 1H), 6.71 (s, 1H), 7.90 (d, $J = 8.1$ Hz, 1H), 7.48 (d, $J = 8.1$ Hz, 1H), 5.0 (s, 3H, -OH); Anal. Calcd for $C_{22}H_{15}ClN_2O_6S$, C= 56.11; H= 3.21; N= 5.95; O= 20.39; Found C= 56.13; H= 3.23; N= 5.97; O= 20.40; ESI MS m/z (% rel. abund.): 470.88 $[M+1]^+$.

4.3.2 4-(6-HYDROXY-4-OXO-4H-CHROMEN-2-YL)-BENZOIC ACID (2,3,4-TRIHYDROXY-BENZYLIDENE)-HYDRAZIDE **2**

M.P. 302°C; Solid; Yield: 75%; 1H NMR (300MHz, DMSO- d_6): 2.0 (s, 1H) 7.81 (s, 1H), 8.11 (s, 1H), 7.48 (s, 1H), 6.75 (s, 1H), 7.21 (s, 1H), 6.84 (s, 1H), 6.71 (s, 1H), 7.90 (d, $J = 8.12$ Hz, 1H), 7.48 (d, $J = 8.11$ Hz, 1H), 5.0 (s, 4H, -OH); Anal. Calcd for $C_{22}H_{15}ClN_2O_6S$, C= 56.11, H= 3.21, N= 5.95, O= 20.39; Found C= 56.12, H= 3.22, N= 5.96, O= 20.40; ESI MS m/z (% rel. abund.): 470.88 $[M+1]^+$.

4.3.3 4-(6-HYDROXY-4-OXO-4H-CHROMEN-2-YL)-BENZOIC ACID (2-HYDROXY-BENZYLIDENE)-HYDRAZIDE **3**

M.P. 302°C; Solid; Yield: 81%; 1H NMR (300MHz, DMSO- d_6) \square 8.1 (s, 1H, -N=CH), 2.0 (s, 1H) 7.79 (d, $J = 8.12$ Hz, 2H), 7.55 (d, $J = 7.89$ Hz, 2H), 6.75 (s, 1H), 7.11 (s, 1H), 6.84 (s, 1H), 6.71 (s, 1H), 7.90 (d, $J = 7.98$ Hz, 1H), 7.48 (d, $J = 8.11$ Hz, 1H), 5.0 (s, 2H, -OH); Anal. Calcd for $C_{22}H_{15}ClN_2O_6S$, C= 56.11, H= 3.21, N= 5.95, O= 20.39, Found C= 56.12, H= 3.22, N= 5.96, O= 20.40, ESI MS m/z (% rel. abund.): 470.8 $[M+1]^+$.

4.3.4 4-(6-HYDROXY-4-OXO-4H-CHROMEN-2-YL)-BENZOIC ACID (3-HYDROXY-BENZYLIDENE)-HYDRAZIDE **4**

M.P. 302°C; Solid; Yield: 91%; 1H NMR (300MHz, DMSO- d_6): 2.0 (s, 1H), 7.76 (d, $J = 7.89$ Hz, 2H),

7.13 (d, $J = 7.42\text{Hz}$, 2H), 6.75 (s, 1H), 7.11 (s, 1H), 6.84 (s, 1H), 6.76 (s, 1H), 7.91 (d, $J = 7.98\text{Hz}$, 1H), 7.48 (d, $J = 7.9\text{Hz}$, 1H), 5.0 (s, 3H, -OH); Anal. Calcd for $\text{C}_{22}\text{H}_{16}\text{N}_2\text{O}_7\text{S}$, C= 58.40; H= 3.56; N= 6.19; O= 24.75; Found C= 58.42; H= 3.57; N= 6.20; O= 24.76; EI MS m/z (% rel. abund.): 400.1 $[\text{M}+1]^+$.

4.3.5 4-(6-HYDROXY-4-OXO-4H-CHROMEN-2-YL)-BENZOIC ACID (4-HYDROXY-BENZYLIDENE)-HYDRAZIDE 5

M.P. 288°C; Solid; Yield: 78%; $^1\text{HNMR}$ (300MHz, $\text{DMSO-}d_6$): 7.4 (s, 1H), 7.49 (s, 1H), 7.37 (s, 1H), 6.7 (s, 1H), 6.75 (s, 1H), 7.11 (s, 1H), 6.84 (s, 1H), 6.71 (s, 1H), 7.90 (d, $J = 7.97\text{ Hz}$, 1H), 7.48 (d, $J = 8.13\text{ Hz}$, 1H), 5.0 (s, 2H, -OH); Anal. Calcd for $\text{C}_{22}\text{H}_{16}\text{N}_2\text{O}_7\text{S}$, C= 58.40; H= 3.56; N= 6.19; O= 24.75; Found C= 58.41; H= 3.57; N= 6.20; O= 24.76; EI MS m/z (% rel. abund.): 452.44 $[\text{M}+1]^+$.

4.3.6 4-(6-HYDROXY-4-OXO-4H-CHROMEN-2-YL)-BENZOIC ACID (4-CHLORO-2-HYDROXY-BENZYLIDENE)-HYDRAZIDE 6

M.P. 342°C; Solid; Yield: 85%; $^1\text{HNMR}$ (300MHz, $\text{DMSO-}d_6$): 7.39 (s, 1H), 7.37 (s, 1H), 7.49 (s, 1H), 6.7 (s, 1H), 6.3 (s, 1H), 6.75 (s, 1H), 7.22 (s, 1H), 6.84 (s, 1H), 6.71 (s, 1H), 7.90 (d, $J = 8.3\text{Hz}$, 1H), 7.48 (d, $J = 7.78\text{Hz}$, 1H), 5.0 (s, 2H, -OH); Anal. Calcd for $\text{C}_{22}\text{H}_{16}\text{N}_2\text{O}_7\text{S}$; C= 58.40; H= 3.56; N= 6.19; O= 24.75; Found C= 58.41; H= 3.57; N= 6.20; O= 24.76; EI MS m/z (% rel. abund.): 452.44 $[\text{M}+1]^+$.

4.3.7 4-(6-HYDROXY-4-OXO-4H-CHROMEN-2-YL)-BENZOIC ACID (2,5-DICHLORO-BENZYLIDENE)-HYDRAZIDE 7

M.P. 336°C; Solid; Yield: 92%; $^1\text{HNMR}$ (300MHz, $\text{DMSO-}d_6$): 7.83 (s, 1H), 7.93 (s, 1H), 8.47 (s, 1H), 7.5 (s, 1H), 6.75 (s, 1H), 7.11 (s, 1H), 6.84 (s, 1H), 6.71 (s, 1H), 7.90 (d, $J = 7.98\text{Hz}$, 1H), 7.57 (d, $J = 7.9\text{Hz}$, 1H), 5.0 (s, 3H, -OH); Anal. Calcd for $\text{C}_{22}\text{H}_{15}\text{N}_3\text{O}_8\text{S}$; C= 54.88; H= 3.14; N= 8.73; O= 26.59; S= 6.60; Found C= 54.89; H= 3.15; N= 8.75; O= 26.60; S= 6.61; ESI MS m/z (% rel. abund.): 481.43 $[\text{M}+1]^+$.

4.3.8 4-(6-HYDROXY-4-OXO-4H-CHROMEN-2-YL)-BENZOIC ACID (2,4-DICHLORO-BENZYLIDENE)-HYDRAZIDE 8

M.P. 304°C; Solid; Yield: 82%; $^1\text{HNMR}$ (300MHz, $\text{DMSO-}d_6$): 7.80 (s, 1H), 8.32 (s, 1H), 8.2 (s, 1H), 8.86 (s, 1H), 6.75 (s, 1H), 7.11 (s, 1H), 6.84 (s, 1H), 6.71 (s, 1H), 7.90 (d, $J = 7.88\text{Hz}$, 1H), 7.48 (d, $J = 7.87\text{Hz}$, 1H), 5.0 (s, 1H, -OH); Anal. Calcd for $\text{C}_{22}\text{H}_{15}\text{N}_3\text{O}_8\text{S}$; C= 54.88; H= 3.14; N= 8.73; O= 26.59; Found C= 54.89; H= 3.15; N= 8.74; O= 26.60; ESI MS m/z (% rel. abund.): 452.12 $[\text{M}+1]^+$ 454.26 $[\text{M}+2]^+$ 481.43 $[\text{M}+4]^+$.

4.3.9 4-(6-HYDROXY-4-OXO-4H-CHROMEN-2-YL)-BENZOIC ACID (2-CHLORO-BENZYLIDENE)-HYDRAZIDE 9

M.P. 288°C; Solid; Yield: 87%; $^1\text{HNMR}$ (300MHz, $\text{DMSO-}d_6$): 2.0 (s, 1H), 8.19 (d, $J = 8.24\text{Hz}$, 2H), 8.47 (d, $J = 8.51\text{Hz}$, 2H), 6.75 (s, 1H), 7.23 (s, 1H), 6.84 (s, 1H), 6.71 (s, 1H), 7.90 (d, $J = 7.98\text{Hz}$, 1H), 7.48 (d, $J = 7.86\text{Hz}$, 1H), 5.0 (s, 1H, -OH); Anal. Calcd for $\text{C}_{22}\text{H}_{15}\text{N}_3\text{O}_8\text{S}$; C= 54.88; H= 3.14; N= 8.73; O= 26.59; Found C= 54.89; H= 3.15; N= 8.75; O= 26.61; ESI MS m/z (% rel. abund.): 481.06 $[\text{M}+1]^+$.

4.3.10 4-(6-HYDROXY-4-OXO-4H-CHROMEN-2-YL)-BENZOIC ACID (3-CHLORO-BENZYLIDENE)-HYDRAZIDE 10

M.P. 297°C; Solid; Yield: 88%; $^1\text{HNMR}$ (300MHz, $\text{DMSO-}d_6$): 2.0 (s, 1H), 7.73 (d, $J = 7.83\text{Hz}$, 2H), 7.3 (s, 1H), 6.75 (s, 1H), 7.22 (s, 1H), 6.84 (s, 1H), 6.71 (s, 1H), 7.90 (d, $J = 8.1\text{Hz}$, 1H), 7.48 (d, $J = 7.67\text{Hz}$, 1H), 5.0 (s, 1H, -OH); Anal. Calcd for $\text{C}_{22}\text{H}_{14}\text{Cl}_2\text{N}_2\text{O}_6\text{S}$; C= 52.29; H= 2.79; N= 5.54; O= 19.00; Found C= 52.30, H= 2.80, N= 5.55 O=19.02; ESI MS m/z (% rel. abund.): 505.33 $[\text{M}+1]^+$.

4.3.11 4-(6-HYDROXY-4-OXO-4H-CHROMEN-2-YL)-BENZOIC ACID (4-CHLORO-BENZYLIDENE)-

HYDRAZIDE 11

M.P. 305°C; Solid; Yield: 82%; ¹HNMR (300MHz, DMSO-*d*₆): 2.0 (s, 1H), 7.87 (s, 1H), 7.43 (s, 1H), 8.10 (s, 1H), 6.75 (s, 1H), 7.23 (s, 1H), 6.84 (s, 1H), 6.71 (s, 1H), 7.91 (d, *J* = 7.98Hz, 1H), 7.48 (d, *J* = 7.85Hz, 1H), 5.0 (s, 1H, -OH); Anal. Calcd for C₂₂H₁₅BrN₂O₆S; C= 51.27; H= 2.93; N= 5.44; O= 18.63; Found C = 51.26, H = 2.91, N = 5.43; ESI MS *m/z* (% rel. abund.): 515.33 [M+1]⁺.

4.3.12 4-(6-HYDROXY-4-OXO-4H-CHROMEN-2-YL)-BENZOIC ACID (4-METHOXY-BENZYLIDENE)-HYDRAZIDE 12

M.P. 315°C; Solid; Yield: 91%; ¹HNMR (300MHz, DMSO-*d*₆): 2.0 (s, 1H), 7.70 (s, 1H), 7.52 (s, 1H), 7.64 (s, 1H), 6.75 (s, 1H), 7.24 (s, 1H), 6.84 (s, 1H), 6.71 (s, 1H), 7.92 (d, *J* = 8.32Hz, 1H), 7.48 (d, *J* = 7.52Hz, 1H), 5.0 (s, 1H, -OH); Anal. Calcd for C₂₄H₁₈N₂O₅, C = 69.56, H = 4.38, N = 6.76; Found C = 69.55, H = 4.37, N = 6.75; ESI MS *m/z* (% rel. abund.): 454.43 [M+1]⁺.

4.3.13 4-(6-HYDROXY-4-OXO-4H-CHROMEN-2-YL)-BENZOIC ACID (3-HYDROXY-4-METHOXY-BENZYLIDENE)-HYDRAZIDE 13

M.P. 315°C; Solid; Yield: 91%; ¹HNMR (300MHz, DMSO-*d*₆): 2.0 (s, 1H), 8.81 (s, 1H), 7.26 (s, 1H), 8.00 (s, 1H), 7.7 (s, 1H), 7.71 (s, 1H), 8.28 (s, 1H), 6.75 (s, 1H), 7.11 (s, 1H), 6.84 (s, 1H), 6.71 (s, 1H), 7.90 (d, *J* = 7.98Hz, 1H), 7.48 (d, *J* = 7.76Hz, 1H), 5.0 (s, 1H, -OH); Anal. Calcd for C₂₅H₁₇N₃O₆S; C= 61.60; H= 3.51; N= 8.62; O= 19.69; Found C = 61.60, H = 3.51, N = 8.62 ; O= 19.70; ESI MS *m/z* (% rel. abund.): 487.48 [M+1]⁺.

4.3.14 4-(6-HYDROXY-4-OXO-4H-CHROMEN-2-YL)-BENZOIC ACID (3,4,5 TRIMETHOXY-BENZYLIDENE)-HYDRAZIDE 14

M.P. 309°C; Solid; Yield: 82%; ¹HNMR (300MHz, DMSO-*d*₆): 2.0 (s, 1H), 7.0 (d, *J* = 7.23 Hz, 2H), 7.2 (s, 1H), 6.75 (s, 1H), 7.11 (s, 1H), 6.84 (s, 1H), 6.71 (s, 1H), 7.90 (d, *J* = 7.94 Hz, 1H), 7.48 (d, *J* = 7.74Hz, 1H), 5.0 (s, 2H, -OH); Anal. Calcd for C₂₀H₁₄N₂O₆S₂; C= 54.29; H= 3.19; N= 6.33; O= 21.70; Found C = 54.30, H = 3.20 N = 6.34; O= 21.71 ESI MS *m/z* (% rel. abund.): 442.46 [M+1]⁺.

4.3.15 4-(6-HYDROXY-4-OXO-4H-CHROMEN-2-YL)-BENZOIC ACID (2-NITRO-BENZYLIDENE)-HYDRAZIDE 15

M.P. 311°C; Solid; Yield: 87%; ¹HNMR (300MHz, DMSO-*d*₆): 2.0 (s, 1H), 7.74 (s, 1H), 7.42 (s, 1H), 7.13 (s, 1H), 7.73 (s, 1H), 2.35 (s, 1H), 6.75 (s, 1H), 7.12 (s, 1H), 6.84 (s, 1H), 6.71 (s, 1H), 7.90 (d, *J* = 7.96Hz, 1H), 7.48 (d, *J* = 7.86Hz, 1H), 5.0 (s, 2H, -OH); Anal. Calcd for C₂₃H₁₈N₂O₆S; C= 61.32; H= 4.03; N= 6.22; O= 21.31; Found C = 61.33, H = 4.04 N = 6.23, O= 21.33; ESI MS *m/z* (% rel. abund.): 450.46 [M+1]⁺.

4.3.16 4-(6-HYDROXY-4-OXO-4H-CHROMEN-2-YL)-BENZOIC ACID (3-NITRO-BENZYLIDENE)-HYDRAZIDE 16

M.P. 303°C; Solid; Yield: 86%; ¹HNMR (300MHz, DMSO-*d*₆): 2.0 (s, 1H), 7.49 (s, 1H), 7.43 (s, 1H), 7.44 (s, 1H), 6.8 (s, 1H), 3.73 (s, 1H), 6.75 (s, 1H), 7.11 (s, 1H), 6.84 (s, 1H), 6.71 (s, 1H), 7.90 (d, *J* = 7.98Hz, 1H), 7.48 (d, *J* = 7.76Hz, 1H), 5.0 (s, 1H, -OH); Anal. Calcd for C₂₃H₁₈N₂O₇S; C= 59.22; H= 3.89; N= 6.01; O= 24.01; Found C = 59.23, H = 3.88 N = 6.03, O= 24.03; ESI MS *m/z* (% rel. abund.): 466.46 [M+1]⁺.

4.3.17 4-(6-HYDROXY-4-OXO-4H-CHROMEN-2-YL)-BENZOIC ACID (4-NITRO-BENZYLIDENE)-HYDRAZIDE 17

M.P. 318°C; Solid; Yield: 62%; ¹HNMR (300MHz, DMSO-*d*₆): 2.0 (s, 1H), 7.32 (d, *J* = 7.45Hz, 2H), 7.67 (d, *J* = 7.86Hz, 2H), 7.95 (s, 1H), 7.99 (s, 1H), 8.34 (s, 1H), 6.75 (s, 1H), 7.11 (s, 1H), 6.84 (s, 1H), 6.71 (s, 1H), 7.90 (d, *J* = 7.98Hz, 1H), 7.48 (d, *J* = 7.86Hz, 1H), 5.0 (s, 1H, -OH); Anal. Calcd for C₂₆H₁₈N₂O₆S; C= 64.19; H= 3.73; N= 5.76; O= 19.73; Found C = 64.21, H = 3.74 N = 5.77 O=19.74; ESI MS *m/z* (% rel. abund.): 486.50 [M+1]⁺.

4.3.18 4-(6-HYDROXY-4-OXO-4H-CHROMEN-2-YL)-BENZOIC ACID (3-HYDROXY-

5-HYDROXYMETHYL-2-METHYL-PYRIDIN-4-METHYLENE-BENZYLIDENE)-HYDRAZIDE 18

M.P. 338°C; Solid; Yield: 78%; ¹HNMR (300MHz, DMSO-*d*₆): 2.0 (s, 1H), 8.20 (s, 1H), 7.60 (s, 1H), 2.35 (s, 1H), 8.74 (s, 1H), 6.75 (s, 1H), 7.23 (s, 1H), 6.84 (s, 1H), 6.71 (s, 1H), 7.90 (d, *J* =7.96Hz, 1H), 7.48 (d, *J* =7.84Hz, 1H), 5.0 (s, 3H, -OH);; Anal. Calcd for C₂₃H₁₇N₃O₈S; C= 55.76; H= 3.46; N= 8.48; O= 25.83; Found C = 55.78, H =3.47, N = 8.49; ESI MS *m/z* (% rel. abund.): 495.46 [M+1]⁺.

4.3.19 4-(6-HYDROXY-4-OXO-4H-CHROMEN-2-YL)-BENZOIC ACID (FURAN-2-YLMETHYLENE)-HYDRAZIDE 19

M.P. 274°C; Solid; Yield: 82%; ¹HNMR (300MHz, DMSO-*d*₆): 2.0 (s, 1H), 2.84 (s, 1H), 6.75 (s, 1H), 7.13 (s, 1H), 6.84 (s, 1H), 6.71 (s, 1H), 7.90 (d, *J* =7.98Hz, 1H), 7.48 (d, *J* = 7.74Hz, 1H), 5.0 (s, 2H, -OH);; Anal. Calcd for C₁₇H₁₄N₂O₆S; C= 54.54; H= 3.77; N= 7.48; O= 25.64 Found C = 54.56, H = 3.78, N = 7.49; ESI MS *m/z* (% rel. abund.): 374.37 [M+1]⁺.

4.3.20 4-(6-HYDROXY-4-OXO-4H-CHROMEN-2-YL)-BENZOIC ACID (5-METHYL-FURAN-2-YLMETHYLENE)-HYDRAZIDE 20

M.P. 282°C; Solid; Yield: 87%; ¹HNMR (300MHz, DMSO-*d*₆): 2.0 (s, 1H), 3.45 (s, 1H), 1.28 (s, 1H), 6.75 (s, 1H), 7.11 (s, 1H), 6.84 (s, 1H), 6.71 (s, 1H), 7.90 (d, *J* =7.98Hz, 1H), 7.48 (d, *J* =7.83Hz, 1H), 5.0 (s, 2H, -OH);; Anal. Calcd for C₁₇H₁₃N₂O₆S; C= 54.69; H= 3.51; N= 7.50; O= 25.71; Found C = 54.67, H = 3.52, N = 7.51; ESI MS *m/z* (% rel. abund.): 373.36[M+1]⁺.

4.4.4 PROFILING OF PHARMACOKINETIC PROPERTIES OF POTENT ALPHA-GLUCOSIDASE INHIBITORS

α -Glucosidase inhibitors were also profiled against p-gp and isozymes of CYP450 through SwissADME tools, this efficiently screened and predicts which compound, can be a substrate or inhibitor of p-gp, and against various CYP450 isozymes. Computational predictive tools are more useful in this regard; P-Glycoprotein invites to focus in pharmaceutical research due to its significant effect on ADME (*Absorption, Distribution, Metabolism, and Excretion*) properties [15]. In our screen compounds (1-18) exhibited low GI absorption, none of the compound showed Pgp substrate and BBB permeability, however compounds 1-6, 11-12 & 15-16 are predicted to be the inhibitors of isozyme CYP1A2, compounds 1-3, 7-17 are predicted to be the inhibitors of isozyme CYP2C9, none of the compound showed inhibition against CYP2D6 while compounds (8, 9, 12, 16 & 18) showed inhibition against CYP3A4 respectively, therefore they can show DDI, drug-drug interactions (Table 4).

Table 4: Pharmacokinetics Properties of Potent α -Glucosidase Inhibitors

Comp #	GI absorption	BBB permeant	Pgp substrate	CYP1 A2 inhibitor	CYP2 C1 inhibitor	CYP2 C9 inhibitor	CYP2 D6 inhibitor	CYP3 A4 inhibitor
1.	Low	No	No	Yes	Yes	Yes	No	No
2.	Low	No	No	Yes	Yes	Yes	No	No
3.	Low	No	No	Yes	Yes	Yes	No	No
4.	Low	No	No	Yes	No	Yes	No	No
5.	Low	No	No	Yes	No	Yes	No	No

6.	Low	No	No	Yes	No	Yes	No	No
7.	Low	No	No	No	Yes	Yes	No	No
8.	Low	No	No	No	Yes	Yes	No	Yes
9.	Low	No	No	No	Yes	Yes	No	Yes
10.	Low	No	No	No	Yes	Yes	No	No
11.	Low	No	No	Yes	Yes	Yes	No	No
12.	Low	No	No	Yes	Yes	Yes	No	Yes
13.	Low	No	No	No	Yes	Yes	No	No
14.	Low	No	No	No	Yes	Yes	No	No
15.	Low	No	No	Yes	Yes	Yes	No	No
16.	Low	No	No	Yes	Yes	Yes	No	Yes
17.	Low	No	No	No	Yes	Yes	No	No
18.	Low	No	No	No	No	Yes	No	Yes
19.	High	No	No	No	No	No	No	No
20.	High	No	No	No	No	Yes	No	No

Mostly compounds are showing high GI absorption, none of the compound showed Pgp substrate and BBB permeation.

4.5 PHYSICOCHEMICAL PROPERTIES PROFILING OF POTENT ALPHA-GLUCOSIDASE INHIBITORS

These are the properties of a molecule deals with, various physicochemical descriptors as examined by *Lipinski et al* for instance, molecular weight (M.Wt) should not be greater than 500 a.m.u, number of hydrogen bond donor (HBD) should be less than 5, number of hydrogen bond acceptor (HBA) less than 10, the octanol / water partition coefficient (log P) should be less than 5, and total polar surface area (TPSA) due to the presence of polar atoms specifically nitrogen “N” and sulphur “S” in the compounds should be within the range of 20-130A² [16]. In our case of study all the screened compounds successfully filtered and showed excellent drug ability properties according to ROF, however compounds 56 & 63 exceeds WLOGP very slightly greater than 5, while compounds all the compounds except 57 slightly exceeds the TPSA greater than 130 A² (Table 5).

Table 5: Physicochemical Properties of Potent α -Glucosidase Inhibitors

Com p #	Formula	M.Wt	Rotatable bonds	Num HB A	Num HB D	Ilogp	WLOGP	TPSAA ²
1.	C ₂₂ H ₁₅ ClN ₂ O ₆ S	470.88	6	7	3	2.17	4.52	134.0
2.	C ₂₂ H ₁₅ ClN ₂ O ₆ S	470.88	6	7	3	2.23	4.52	134.0
3.	C ₂₂ H ₁₅ ClN ₂ O ₆ S	470.88	6	7	3	2.57	4.52	134.0
4.	C ₂₂ H ₁₆ N ₂ O ₇ S	452.44	6	8	4	2.20	3.58	154.3
5.	C ₂₂ H ₁₆ N ₂ O ₇ S	452.44	6	8	4	1.69	3.58	154.3
6.	C ₂₂ H ₁₆ N ₂ O ₇ S	452.44	6	8	4	1.69	2.60	154.3
7.	C ₂₂ H ₁₅ N ₃ O ₈ S	481.43	7	9	3	0.56	3.78	179.9
8.	C ₂₂ H ₁₅ N ₃ O ₈ S	481.43	7	9	3	1.77	3.78	179.9
9.	C ₂₂ H ₁₅ N ₃ O ₈ S	481.43	7	9	3	1.91	3.78	179.9
10.	C ₂₂ H ₁₄ Cl ₂ N ₂ O ₆ S	505.33	6	7	3	2.45	5.18	134.0
11.	C ₂₂ H ₁₅ BrN ₂ O ₆ S	515.33	6	7	3	3.13	4.58	91.90
12.	C ₂₂ H ₁₅ FN ₂ O ₆ S	454.43	6	8	3	2.22	4.43	134.0
13.	C ₂₅ H ₁₇ N ₃ O ₆ S	487.48	6	8	3	2.29	3.64	146.9
14.	C ₂₀ H ₁₄ N ₂ O ₆ S ₂	442.46	6	7	3	1.66	4.42	162.3
15.	C ₂₃ H ₁₈ N ₂ O ₆ S	450.46	6	7	3	2.88	4.18	134.0
16.	C ₂₃ H ₁₈ N ₂ O ₇ S	466.46	7	8	3	2.44	3.88	143.3
17.	C ₂₆ H ₁₈ N ₂ O ₆ S	486.50	6	7	3	2.53	5.02	134.0

IHIBITORS

18.	C ₂₃ H ₁₇ N ₃ O ₈ S	495.46	7	9	3	2.29	4.09	179.9
19.	C ₁₇ H ₁₄ N ₂ O ₆ S	374.37	5	7	3	1.73	2.44	134.0
20.	C ₁₈ H ₁₆ N ₂ O ₆ S	388.39	6	7	3	1.91	2.83	134.0

All the compounds are showing excellent drug ability properties according to ROF.

4.6 BRAIN OR INTESTINAL ESTIMATE D PERMEATION (BOILED-EGG)

Drug absorption through human gastrointestinal tract and penetration across the blood brain barriers are the two pharmacokinetics behavior with pivotal importance to be estimate, therefore the develop Brain or Intestinal Estimate D permeation (BOILED-Egg) method is proposed as an accurate predictive model which efficiently works through computing the lipophilicity and polarity behavior of small organic molecules [17]. It is a plot b/w WLOGP, and TPSA (Total Polar Surface Area). Those compounds which exist in the yellow (egg yolk) region have high probability of blood brain barrier permeation, while those compounds which exists in the egg white region have high probability of absorption through gastrointestinal tract, in our screened compounds all the inhibitors are lying within Egg white region and predicted to be absorbed by Gastrointestinal tract, while none of the compound is lying within Egg yolk yellow region therefore not to be permeate by BBB of the Boiled egg region and also predicted not to be effluated from CNS by p-glycoprotein. Figure 6 Showing all the compounds are lying within Egg white region.

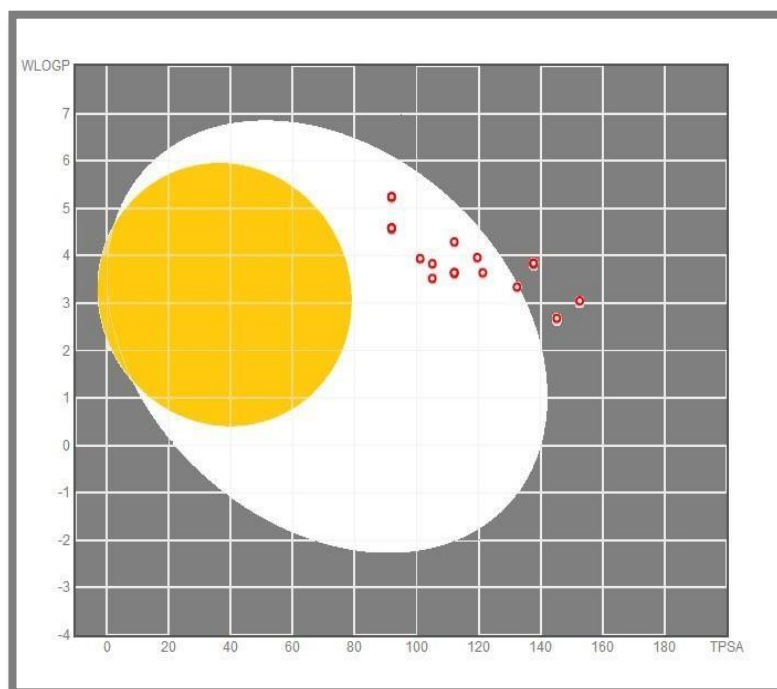
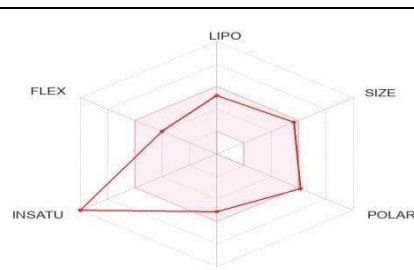
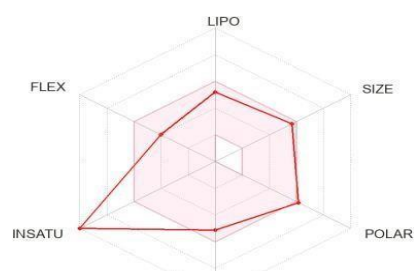
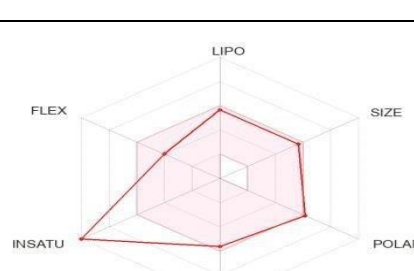
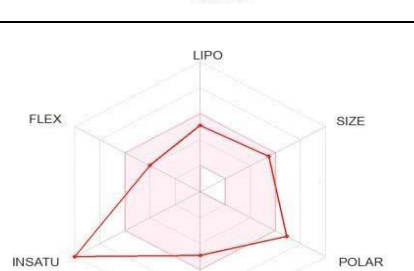


Figure 6: Showing all the compounds are lying within Egg white region and predicted to be absorbed by Gastrointestinal tract, while none of the compound is lying within Egg Yolk region therefore not to be permeate by BBB of the Boiled egg region and predicted not to be effluated from CNS by p-glycoproteins

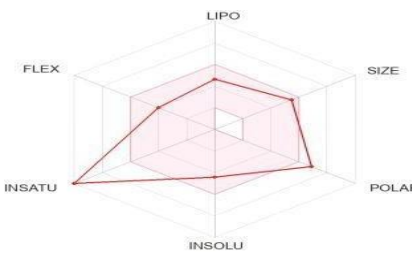
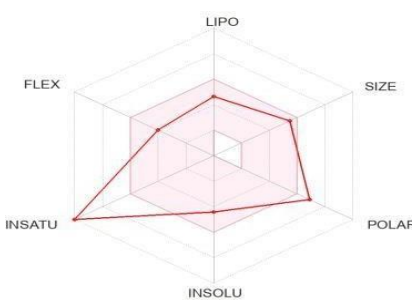
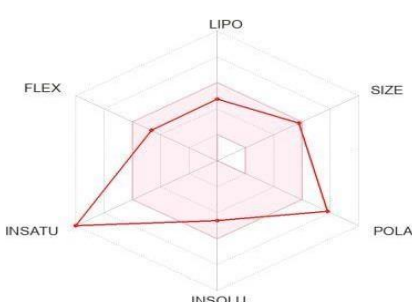
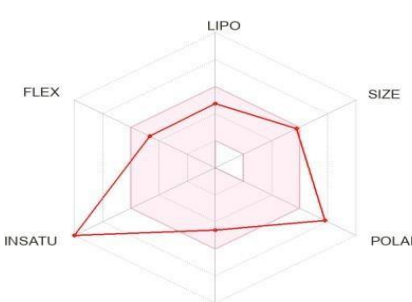
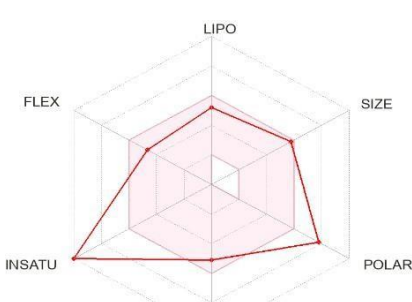
4.7 MAPPING OF BIOAVAILABILITY RADAR OF POTENT ALPHA-GLUCOSIDASE INHIBITORS

Drugs mapping by using bioavailability radar display *drug-likeness* properties of a molecule at a glance, it is the descriptor of six properties, (*LIPO*, *SIZE*, *POLAR*, *INSOLU*, *INSATU*, *FLEX*), the highlighted pink area represents the optimal range of each descriptor, those molecules which exist within the pink area are considered to have good bioavailability in the body [18] All the screened compounds are displaying the acceptable five properties of descriptors, except the descriptor of *INSATU* due to the presence of increase instauration (Table 7).

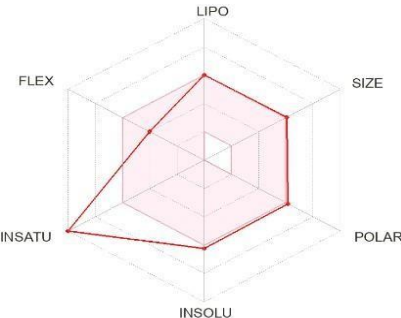
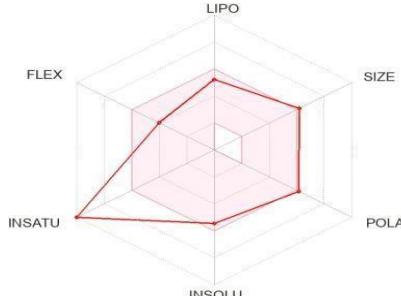
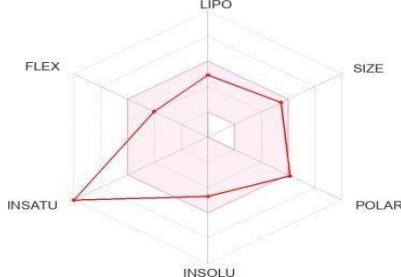
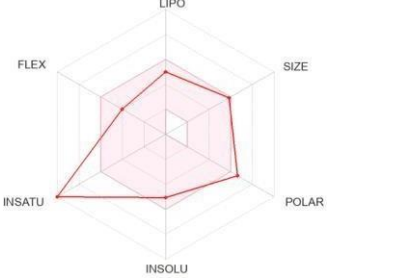
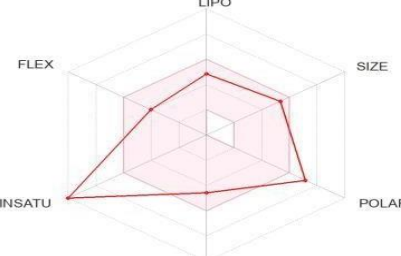
Table 7: Bioavailability Radar of Potent α -Glucosidase Inhibitors

Comp #	Bioavailability Radar	LIPO	SIZE	POLAR	INSOLU	INSATU	FLEX
1.		FPR	FPR	FPR	FPR	SH	FPR
2.		FPR	FPR	FPR	FPR	SH	FPR
3.		FPR	FPR	FPR	FPR	SH	FPR
4.		FPR	FPR	FPR	FPR	SH	FPR

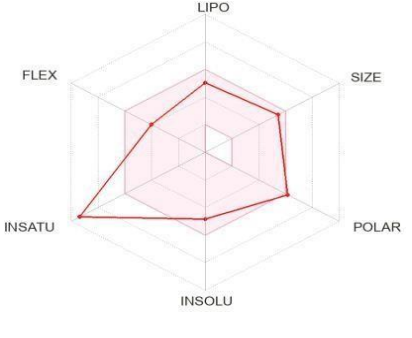
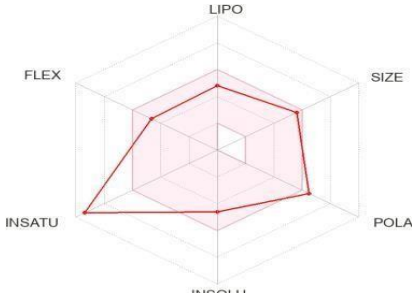
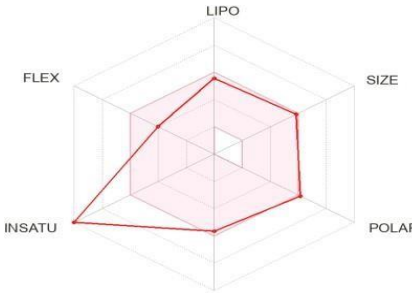
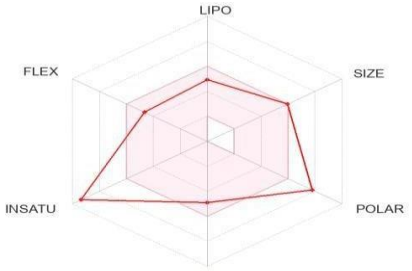
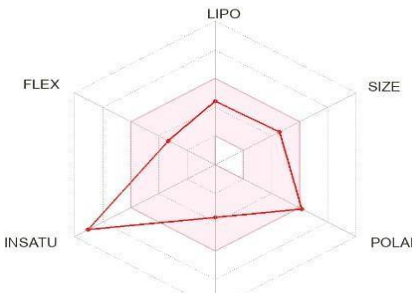
IHIBITORS

5.		FPR	FPR	FPR	FPR	SH	FPR
6.		FPR	FPR	FPR	FPR	SH	FPR
7.		FPR	FPR	FPR	FPR	SH	FPR
8.		FPR	FPR	FPR	FPR	SH	FPR
9.		FPR	FPR	FPR	FPR	SH	FPR

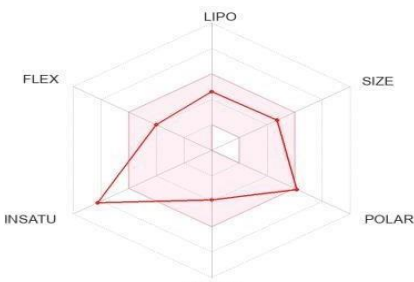
IHIBITORS

10.		FPR	FPR	FPR	FPR	SH	FPR
11.		FPR	FPR	FPR	FPR	SH	FPR
12.		FPR	FPR	FPR	FPR	SH	FPR
13.		FPR	FPR	FPR	FPR	SH	FPR
14.		FPR	FPR	FPR	FPR	SH	FPR

IHIBITORS

15.		FPR	FPR	FPR	FPR	SH	FPR
16.		FPR	FPR	FPR	FPR	SH	FPR
17.		FPR	FPR	FPR	FPR	SH	FPR
18.		FPR	FPR	FPR	FPR	SH	FPR
19.		FPR	FPR	FPR	FPR	SH	FPR

IHIBITORS

20.		FPR	FPR	FPR	FPR	SH	FPR
-----	---	-----	-----	-----	-----	----	-----

All compounds are showing good bioavailability radar of 5 descriptors; however, the sixth descriptor of instauration is slightly increased in all compounds.

4.8 ANTI-OXIDANT (DPPH RADICAL SCAVENGING) ACTIVITY FLAVONE HYDRAZIDE SULFONYL DERIVATIVES 1-20

In order to investigate the anti-oxidant activity all, the synthesized derivatives 47–66 were subjected for the evaluation of anti-oxidant activity (Table 8). The results were compared with standard *Tert.*Butyl 4-Hydroxynisole ($IC_{50} = 44.7 \pm 0.14$ mM). All these compound showed very promising anti-oxidant activity with IC_{50} ranges 15.25–78.22 mM and found to be better active than the standard *Tert.*Butyl 4-Hydroxynisole.

Table 8: Anti-oxidant (DPPH radical scavenging) activity of Compounds 1-20

S.#	$IC_{50} \mu M \pm SEM^a$	S.#	$IC_{50} \mu M \pm SEM^a$
1.	42.22 ± 1.35	11.	57.22 ± 1.47
2.	46.56 ± 1.78	12.	34.28 ± 1.55
3.	44.88 ± 1.44	13.	39.1 ± 1.22
4.	18.23 ± 1.68	14.	41.88 ± 1.67
5.	16.72 ± 1.89	15.	68.43 ± 1.22
6.	15.25 ± 1.32	16.	48.5 ± 1.55
7.	52.11 ± 0.87	17.	54.24 ± 1.11
8.	58.46 ± 1.12	18.	64.23 ± 1.73
9.	49.23 ± 1.64	19.	78.22 ± 1.42
10.	58.23 ± 1.66	20.	77.35 ± 1.65
	<i>Tert.</i> Butyl4-Hydroxynisole (Standard)		44.7 ± 0.14

^aSEM = Standard Error Mean

The –OH group containing compounds **4** ($IC_{50} = 18.23 \pm 1.68 \mu M$), **5** ($IC_{50} = 16.72 \pm 1.89 \mu M$), **6** ($IC_{50} = 15.25 \pm 1.32 \mu M$), better activity among their look likes. The highest activity shown by compound **6** ($IC_{50} = 15.25 \pm 1.32 \mu M$). While 3rd most active compound **4** ($IC_{50} = 18.23 \pm 1.6 \mu M$). The chloro (-Cl) substituted compounds **1** ($IC_{50} = 42.22 \pm 1.35 \mu M$), **2** ($IC_{50} = 46.56 \pm 1.78 \mu M$), **3** ($IC_{50} = 44.88 \pm 1.44 \mu M$) and **10** ($IC_{50} = 58.23 \pm 1.66 \mu M$) also showed significant activity towards α -glucosidase inhibition. All these compounds showed better activity than the standard. The –NO₂ group substituted compounds **7** ($IC_{50} = 52.11 \pm 0.87 \mu M$), **8** ($IC_{50} = 58.46 \pm 1.12 \mu M$), **9** ($IC_{50} = 49.23 \pm 1.64 \mu M$) were also found to be better active than the standard but relatively they showed less activity than –OH group containing analogues. The less activity might be due to reducing number of hydrogen bonding interaction sites or larger size of –NO₂ group than the –OH group.

Compound containing –CH₃ and OCH₃ group substituted **15** ($IC_{50} = 68.43 \pm 1.22 \mu M$), **16** ($IC_{50} = 48.5 \pm 1.55 \mu M$) and **18** ($IC_{50} = 64.23 \pm 1.73 \mu M$) show slightly less active than the standard. The heterocyclic ring containing compounds **13** ($IC_{50} = 39.1 \pm 1.22 \mu M$) and **14** ($IC_{50} = 41.88 \pm 1.67 \mu M$) showed better activity and they were also found to be better active than the standard but compound **17** ($IC_{50} = 54.24 \pm 1.11 \mu M$) showed less active than standard. The halogen containing compounds **11** ($IC_{50} = 57.22 \pm 1.47 \mu M$) and **12** ($IC_{50} = 34.28 \pm 1.55 \mu M$) showed better activity and they were also found to be better active than the standard.

5. Conclusion

Flavone Hydrazide Sulfonyl Derivatives **1-20** has synthesized and evaluated for their α -glucosidase inhibition activity. These compounds showed remarkable inhibition activity. According to molecular docking results, these molecules can interact with the protein molecule through π - π and H-bonding

interactions. Furthermore, the pharmacokinetic, physicochemical, Brain or Intestinal Estimated Permeation (BOILED-Egg) and bioavailability radar studies were investigated studies by computational analysis. These studies revealed that the synthesized compounds **1-20** have high Gastrointestinal (GI) absorption with excellent values of various parameters required to best fit for Lipinski rule for drug likeness The Brain or Intestinal Estimated Permeation (BOILED-Egg) study predicted that all of the compounds are located in the egg white region and will be absorbed by the gastrointestinal tract and will not be able to absorbed by *the p*-glycoproteins and will not permeated by the blood-brain barrier. Additionally, the analysis of the bioavailability radar shown that all compounds exhibited good bioavailability radar of five descriptors; however, a slight increase in instauration (the sixth descriptor). Therefore, this study explored the excellent α -glucosidase inhibitors with special structural pharmacophore features. Thus, these derivatives can be used in the process of drug developing process for as anti-diabetic medications.

6. Materials and methods

All nuclear magnetic resonance tests were conducted at 150 and 300 MHz using an Advance Bruker apparatus. The Perkin Elmer 2400-II CHNS/O Elemental Analyzer in the United States and the Finnigan MAT-311A in Germany were used for elemental analysis and electron impact mass spectra (EI-MS), respectively.

References

- [1] L. Chen, D. J. Magliano, and P. Z. Zimmet, "The worldwide epidemiology of type 2 diabetes mellitus - Present and future perspectives," *Nature Reviews Endocrinology*, vol. 8, no. 4. pp. 228–236, Apr. 2012. doi: 10.1038/nrendo.2011.183.
- [2] M. Finucane *et al.*, "National, regional, and global trends in fasting plasma glucose and diabetes prevalence since 1980: systematic analysis of health examination surveys and epidemiological studies with 370 country-years and 2.7 million participants," *Lancet*, vol. 378, pp. 31–40, 2011, doi: 10.1016/S0140.
- [3] World Health Organization and International Diabetes Federation, *Definition and diagnosis of diabetes mellitus and intermediate hyperglycaemia : report of a WHO/IDF consultation*.
- [4] Y. Zheng, S. H. Ley, and F. B. Hu, "Global aetiology and epidemiology of type 2 diabetes mellitus and its complications," *Nature Reviews Endocrinology*, vol. 14, no. 2. Nature Publishing Group, pp. 88–98, 2018. doi: 10.1038/nrendo.2017.151.
- [5] R. Malek, S. Hannat, A. Nechadi, F. Z. Mekideche, and M. Kaabeche, "Diabetes and Ramadan: A multicenter study in Algerian population," *Diabetes Research and Clinical Practice*, vol. 150. Elsevier Ireland Ltd, pp. 322–330, Apr. 01, 2019. doi: 10.1016/j.diabres.2019.02.008.
- [6] Y. J. Choi and Y.-S. Chung, "Type 2 diabetes mellitus and bone fragility: Special focus on bone imaging," *Osteoporos. Sarcopenia*, vol. 2, no. 1, pp. 20–24, 2016, doi: 10.1016/j.afos.2016.02.001.
- [7] A. K. Picke, G. Campbell, N. Napoli, L. C. Hofbauer, and M. Rauner, "Update on the impact of type 2 diabetes mellitus on bone metabolism and material properties," *Endocrine Connections*, vol. 8, no. 3. BioScientifica Ltd., pp. R55–R70, 2019. doi: 10.1530/EC-18-0456.
- [8] R. M. Carrillo-Larco, N. C. Barengo, L. Albitres-Flores, and A. Bernabe-Ortiz, "The risk of mortality among people with type 2 diabetes in Latin America: A systematic review and metaanalysis of population-based cohort studies," *Diabetes. Metab. Res. Rev.*, vol. 35, no. 4, pp. 1– 11, 2019, doi: 10.1002/dmrr.3139.

- [9] H. Ali, P. J. Houghton, and A. Soumyanath, “ α -Amylase inhibitory activity of some Malaysian plants used to treat diabetes; with particular reference to *Phyllanthus amarus*,” *J. Ethnopharmacol.*, vol. 107, no. 3, pp. 449–455, 2006, doi: 10.1016/j.jep.2006.04.004.
- [10] M. R. Bhandari, N. Jong-Anurakkun, G. Hong, and J. Kawabata, “ α -Glucosidase and α -amylase inhibitory activities of Nepalese medicinal herb Pakhanbhed (*Bergenia ciliata*, Haw.),” *Food Chem.*, vol. 106, no. 1, pp. 247–252, 2008, doi: 10.1016/j.foodchem.2007.05.077.
- [11] S. A. Adefegha and G. Oboh, “Inhibition of key enzymes linked to type 2 diabetes and sodium nitroprusside-induced lipid peroxidation in rat pancreas by water extractable phytochemicals from some tropical spices,” *Pharm. Biol.*, vol. 50, no. 7, pp. 857–865, 2012, doi: 10.3109/13880209.2011.641022.
- [12] S. Poovitha and M. Parani, “In vitro and in vivo α -amylase and α -glucosidase inhibiting activities of the protein extracts from two varieties of bitter melon (*Momordica charantia* L.),” *BMC Complement. Altern. Med.*, vol. 16, no. Suppl 1, pp. 1–8, 2016, doi: 10.1186/s12906-016-1085-1.
- [13] O. Trott and A. J. Olson, “AutoDock Vina: Improving the speed and accuracy of docking with a new scoring function, efficient optimization, and multithreading,” *J. Comput. Chem.*, vol. 31, no. 2, p. NA-NA, 2009, doi: 10.1002/jcc.21334.
- [14] J. Eberhardt, D. Santos-Martins, A. F. Tillack, and S. Forli, “AutoDock Vina 1.2.0: New Docking Methods, Expanded Force Field, and Python Bindings,” *J. Chem. Inf. Model.*, vol. 61, no. 8, pp. 3891–3898, 2021, doi: 10.1021/acs.jcim.1c00203.
- [15] A. Allouche, “Software News and Updates Gabedit — A Graphical User Interface for Computational Chemistry Softwares,” *J. Comput. Chem.*, vol. 32, pp. 174–182, 2012, doi: 10.1002/jcc.
- [16] A. M. Dar and S. Mir, “Molecular Docking: Approaches, Types, Applications and Basic Challenges,” *J. Anal. Bioanal. Tech.*, vol. 08, no. 02, pp. 8–10, 2017, doi: 10.4172/21559872.1000356.
- [17] A. Daina and V. Zoete, “A BOILED-Egg To Predict Gastrointestinal Absorption and Brain Penetration of Small Molecules,” *ChemMedChem*, pp. 1117–1121, 2016, doi: 10.1002/cmdc.201600182.
- [18] A. Daina, O. Michielin, and V. Zoete, “SwissADME: A free web tool to evaluate pharmacokinetics, drug-likeness and medicinal chemistry friendliness of small molecules,” *Sci. Rep.*, vol. 7, Mar. 2017, doi: 10.1038/srep42717.